Optical and electrical characterizations of nanoparticle Cu_2S thin films

M. Saadeldin[a)], H. S. Soliman[b)], H. A. M. Ali[b)], and K. Sawaby[a)†]

[a)] *Physics Department, Faculty of Science, Cairo University, Giza* 12613, *Egypt*

[b)] *Physics Department, Faculty of Education, Ain-Shams University, Cairo* 11757, *Egypt*

(Received 22 June 2013; revised manuscript received 10 September 2013; published online 20 February 2014)

Copper sulfide thin films are deposited onto different substrates at room temperature using the thermal evaporation technique. X-ray diffraction spectra show that the film has an orthorhombicchalcocite (γ-Cu_2S) phase. The atomic force microscopy images indicate that the film exhibits nanoparticles with an average size of nearly 44 nm. Specrtophotometric measurements for the transmittance and reflectance are carried out at normal incidence in a spectral wavelength range of 450 nm–2500 nm. The refractive index, n, as well as the absorption index, k is calculated. Some dispersion parameters are determined. The analyses of ε_1 and ε_2 reveal several absorption peaks. The analysis of the spectral behavior of the absorption coefficient, α, in the absorption region reveals direct and indirect allowed transitions. The dark electrical resistivity is studied as a function of film thickness and temperature. Tellier's model is adopted for determining the mean free path and bulk resistance.

Keywords: physical properties of Cu_2S thermal evaporation, nanoparticle Cu_2S thin films

PACS: 68.35.bg **DOI:** 10.1088/1674-1056/23/4/046803

1. Introduction

Copper sulfide thin films have received ever-increasing attention due to their wide variety of applications, such as solar cell, optoelectronic devices, solar tubular solar collectors,[1] electro conductive coating,[2] microwave shielding coating and sensors.[3] Copper sulfides (Cu_xS, $1 \leq x \leq 2$) are interesting materials because of their semiconducting properties.[4] As is well known, they are a p-type defect semiconductors with shallow Cu vacancy acceptors.[5] Indeed, the variation in x, $1 \leq x \leq 2$, can provide a range of distinct crystalline phases depending on the temperature, producing significant variation in the electrical conductivity.[4] In addition, their optical properties depend on the size and shape of copper sulfides. Thus, it is important to control their morphologies and compositions for application in optoelectrical devices. However, there have been a few reports on the detailed controls of the morphology and composition of copper sulfide.[6]

In the present study, the structural, morphological, and optical properties of Cu_2S thin films prepared by thermal evaporation technique are investigated using X-ray diffraction (XRD), atomic force microscopy (AFM), and spectrophotometric measurements.

2. Experimental technique

Copper sulfide (Cu_2S) thin films were prepared by the thermal evaporation technique in a vacuum (1.33×10^{-3} Pa) from high purity Cu_2S powder (99.9%) using a vacuum coating unit system (Edwards, 306A). A tungsten boat was used as the evaporation source and the substrates were glass and quartz, which were held at room temperature. The film deposition rate was kept at 2.5 nm·s^{-1}. The thickness was measured by using the thickness monitors (model FTM4, Edwards Co. England) and an optical interference based on the Tolansky's method.[7] The film thickness values were in a range from 113 nm to 453 nm. A Philips X-ray diffractometer (model X′ pert with monochromatic Cu Kα, operated at 40 kV and 25 mA) was used to carry out the XRD study on Cu_2S thin films at room temperature. The AFM contact mode with silicon tips was used to investigate the surface morphologies of the investigated films. For the optical properties, the transmission $T(\lambda)$ and the reflection $R(\lambda)$ of the films were measured at normal incidence of light in a spectral range of 450 nm–2500 nm using a double beam spectrophotometer (JASCO, V-570 UV-VIS-NIR). The absolute values of the measured transmittance and reflectance, after correction of the absorbance and reflectance of the substrate, are given by[8,9]

$$T = (I_{\rm ft}/I_{\rm q})(1 - R_{\rm q}), \tag{1}$$

where $I_{\rm ft}$ and $I_{\rm q}$ are the intensities of light passing, respectively, through the film-quartz system and through the reference quartz, and $R_{\rm q}$ is the reflectance of quartz, and

$$R = (I_{\rm fr}/I_{\rm m})R_{\rm m}[1 + (1 - R_{\rm q})^2] - T^2 R_{\rm q}, \tag{2}$$

where $I_{\rm fr}$ is the intensity of light reflected from the sample reaching the detector, $I_{\rm m}$ is the intensity of light reflected from the reference mirror, and $R_{\rm m}$ is the mirror reflectance.

From the values of T, R, and the film thickness d, the values of refractive index n and absorption coefficient k are

†Corresponding author. E-mail: phy_kamel@yahoo.com

© 2014 Chinese Physical Society and IOP Publishing Ltd

computed by a special computer program[10,11] based on minimizing $(\Delta T)^2$ and $(\Delta R)^2$ simultaneously, where

$$(\Delta T)^2 = |T_{(n,k)} - T|^2, \quad (3)$$

$$(\Delta R)^2 = |R_{(n,k)} - R|^2, \quad (4)$$

where $T_{(n,k)}$ and $R_{(n,k)}$ are the calculated values of T and R using the Murmann's exact equations. The experimental errors in measuring the film thickness are taken to be $\pm 2\%$ in T and $\pm 1\%$ in R, and the errors in the calculated values of n and k are estimated to be 3% and 2.5%, respectively.

For electrical measurements, the dark electrical resistivity, ρ, of Cu_2S thin film was measured by a high internal impedance electrometer (Keithely 617A) based on the two probe method in a temperature range from 303 K to 423 K. The temperatures of the films were measured using a chromel-alumel thermocouple. The Ohmic contacts were made by evaporating gold electrodes.

3. Results and discussion

3.1. Structural characterization

The X-ray diffractiometry method was used to obtain the structural characterizations. Figure 1 shows the XRD patterns for the prepared Cu_2S thin film with a thickness of 453 nm. The pattern is characterized by many diffraction lines existing with a broad hump in a 2θ range from 20° to 35°. Thus, the film exhibits a nanocrystalline and polycrystalline nature. By comparing the observed XRD patterns for the prepared copper sulfide thin film with the data on the ICDD-card number 09-0328 (standard JCPDS card), the values of Miller index (hkl) and lattice spacing (d), each of which is corresponding respectively to a diffraction line in the XRD pattern of Cu_2S thin film, are indexed and collected in Table 1. In addition, the prepared film of Cu_2S reveals that the film possesses a structure that matches the orthorhombic crystal system with lattice constant ($a = 11.83$ Å, $b = 27.05$ Å, $c = 13.43$ Å). This result is consistent with that observed in orthorhombic chalcocite (γ-Cu_2S) phase.[12,13]

The AFM technique provides a direct observation of the surface morphology of the prepared film. The two-dimensional (2D) and three-dimensional (3D) AFM images of the Cu_2S film are shown in Figs. 2(a) and 2(b). The film exhibits nanoparticles with an average size of nearly 44 nm.

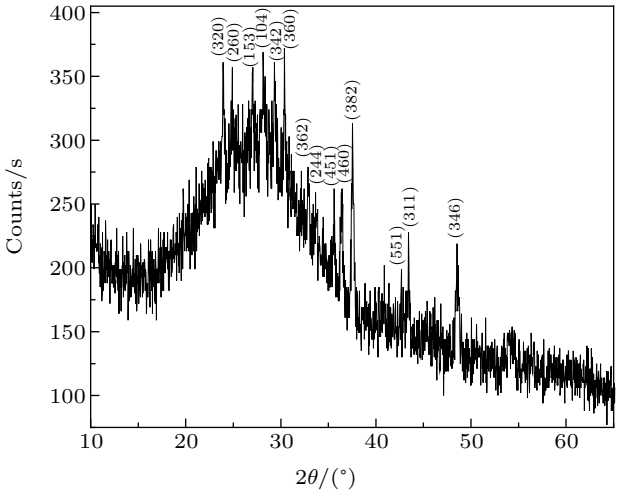


Fig. 1. XRD patterns of Cu_2S thin film with a thickness of 453 nm.

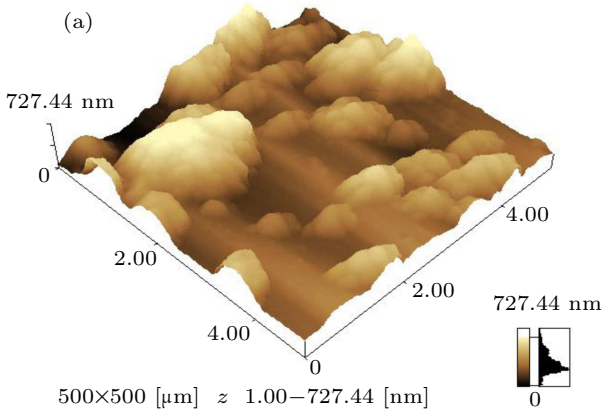




Fig. 2. (color online) 2D (a) and 3D (b) AFM images for Cu_2S thin film.

Table 1. Analysis of XRD patterns of Cu_2S thin film by comparing the data on the ICDD-card number 09-0328.

d-space	3.7139	3.5731	3.2990	3.1617	3.0387	2.9398	2.7193	2.6599	2.5177	2.4659	2.3930	2.1175	2.0816	1.8764
$2\theta/(^\circ)$	23.9	24.89	27	28.2	29.36	30.37	32.78	33.66	35.6	36.4	37.5	42.66	43.43	48.47
(hkl)	320	260	153	104	342	360	362	244	451	460	382	551	311	346

3.2. Optical characterization

The optical properties of Cu_2S thin films were determined from transmittance, $T(\lambda)$ and reflectance, $R(\lambda)$ measurements in a range of 450 nm–2500 nm. Figure 3 shows the spectral distributions of $T(\lambda)$ and $R(\lambda)$ for Cu_2S film with a thickness 453 nm, as a representative example. The Cu_2S

film exhibits high transmittance at longer wavelength in the near-infrared region. The transmittance in this region may be due to the free carriers. While the transmittance in the shorter wavelength is attributed to the interband transition from the valence band to the conduction band. The spectral behavior of the reflectance of Cu_2S film reveals three peaks at 600, 780, and 1240 nm.

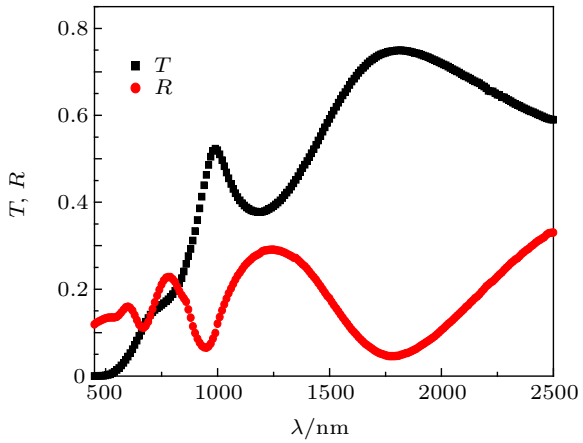


Fig. 3. (color online) Spectral distributions of transmittance, $T(\lambda)$ and reflectance $R(\lambda)$ of Cu_2S thin film with a thickness of 453 nm as a representative example.

The dispersion curve of the refractive index for Cu_2S film is shown in Fig. 4. The curve shows the anomalous dispersion in the refractive index spectrum, at $\lambda < 1000$ nm, which can be explained by using the multi-oscillator model.[14] The normal dispersion is observed at $\lambda > 1000$ nm, to which a single oscillator model can be applied.

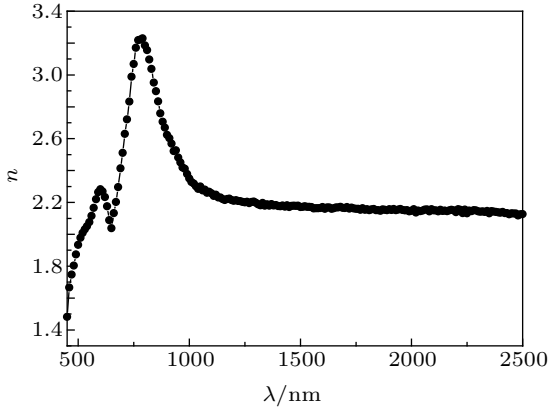


Fig. 4. Dispersion curve of the refractive index $n(\lambda)$ of Cu_2S film.

In the single oscillator model, which was given by Didomenico and Wemple[15,16], the refractive index, n, is related to the dispersion parameters (E_o and E_d) by

$$n^2 - 1 = E_o E_d / [E_o^2 - (E)^2], \tag{5}$$

where E is the photon energy $h\upsilon$, E_o is the single oscillator energy and E_d is the dispersion energy, E_o and E_d are directly determined from the slope $(E_o E_d)^{-1}$ and the intersection (E_o/E_d) with the vertical axis. The calculated values of E_o and E_d are 3.22 eV and 11.23 eV. A plot of $(n^2-1)^{-1}$ versus $(h\upsilon)^2$ of Cu_2S thin film is illustrated in Fig. 5. The refractive index $n(0)$ at zero photon energy, which is defined by the infinite wavelength dielectric constant ε_∞, can be deduced to be 4.474, from the dispersion relationship by extrapolation of the linear part.

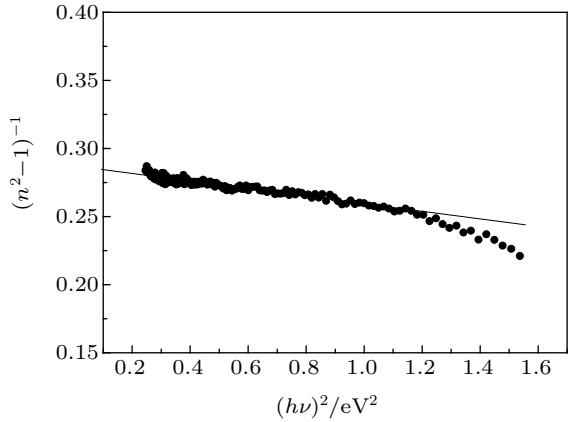


Fig. 5. Plot of $(n^2-1)^{-1}$ versus $(h\nu)^2$ of Cu_2S thin film.

The relation between the lattice dielectric constant ε_L, and the refractive index (n) is given by[17]

$$n^2 = \varepsilon_L - (1/4\pi^2\varepsilon_o)(e/c)^2(N/m^*)\lambda^2, \tag{6}$$

where N/m^* is the ratio of the carrier concentration to the effective mass, c is the speed of light, and e is the electronic charge. The plot of n^2 versus λ^2 is shown in Fig. 6. The values of ε_L and N/m^* are determined from the extrapolation of the plot at $\lambda^2 = 0$ and from the slope of the graph. The obtained values are 4.79 and 4.84×10^{55} $\mathrm{m}^{-3}\cdot\mathrm{kg}^{-1}$ for ε_L and N/m^*, respectively.

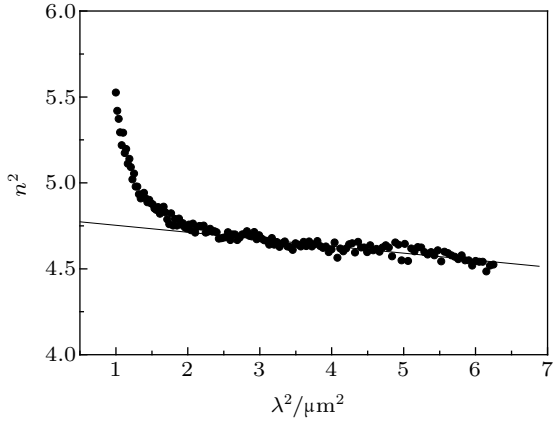


Fig. 6. Plot of n^2 versus $(\lambda)^2$ of Cu_2S thin film.

The real part (ε_1) and imaginary (ε_2) part of the dielectric constant are determined using the following relation:[18,19]

$$\varepsilon = \varepsilon_1 + i\varepsilon_2, \tag{7}$$

where $\varepsilon_1 = n^2 - k^2$ and $\varepsilon_2 = 2nk$.

The real part generally relates to dispersion, while the imaginary part provides a measure of dissipative rate of the wave in a medium.[20] Figure 7 shows the variations of ε_1 and ε_2 with the incident photon energy for Cu_2S film. The spectrum of the real part of the dielectric constant exhibits two peaks at 1.58 eV and 2.06 eV, while the spectrum of its imaginary part exhibits three peaks at 1.05, 1.61, and 2.33, respectively

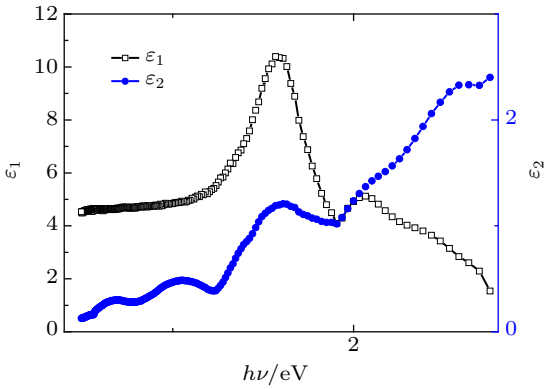


Fig. 7. (color online) Variations of real part (ε_1) and imaginary part (ε_2) of dielectric constant with photon energy of Cu_2S thin film.

The absorption coefficient, α, is calculated from the average absorption index as $4\pi k/\lambda$. The spectral behavior of the absorption coefficient as a function of energy, $h\upsilon$, is shown in Fig. 8. To obtain the information about direct or indirect interband transition, the fundamental absorption edge data could be analyzed within the framework of one electron theory of Bardeen *et al.*[21] This theory can be used to analyze the absorption edge data of the semiconducting solids:[22]

$$(\alpha h\upsilon) = A(h\upsilon - E_g)^r, \tag{8}$$

where A is a constant, h is the Planck's constant, E_g is the energy band gap and r is a parameter whose values may be $1/2$, 2, $3/2$, and 3 which are related to the allowed-direct, allowed-indirect, forbidden-direct, and forbidden-indirect optical transitions, respectively. The plots of $(\alpha h\upsilon)^{1/r}$ versus $h\upsilon$ for different values of straight line fittings at $r = 1/2$ and 2 are shown in Figs. 9(a) and 9(b), respectively. Thus, both direct- and indirect-allowed transitions are exhibited for the Cu_2S film. The energy gaps are found to be 2.266 eV and 1.034 eV for the direct-allowed transition and indirect-allowed transition, respectively. These results are consistent with those given by Mulder in Ref. [23], who suggested a band model with two types of transitions: indirect at around 1.2 eV and direct in the range of 2 eV–2.5 eV. Table 2 gives the values of energy gap obtained in the present work and other study[24] for comparison. Different values of energy gap may be due to different techniques of preparation and also to the mechanism of the light absorption in the film.

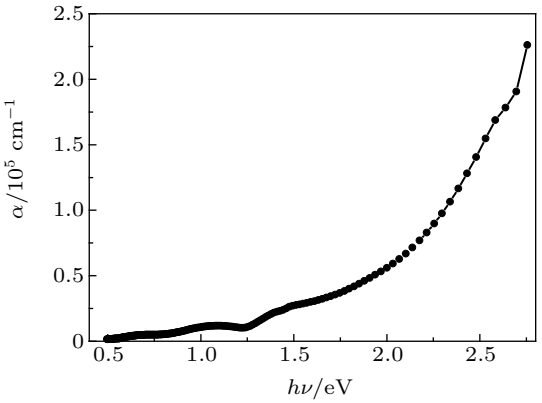


Fig. 8. Spectral behavior of the absorption coefficient (α) with respect to the photon energy.

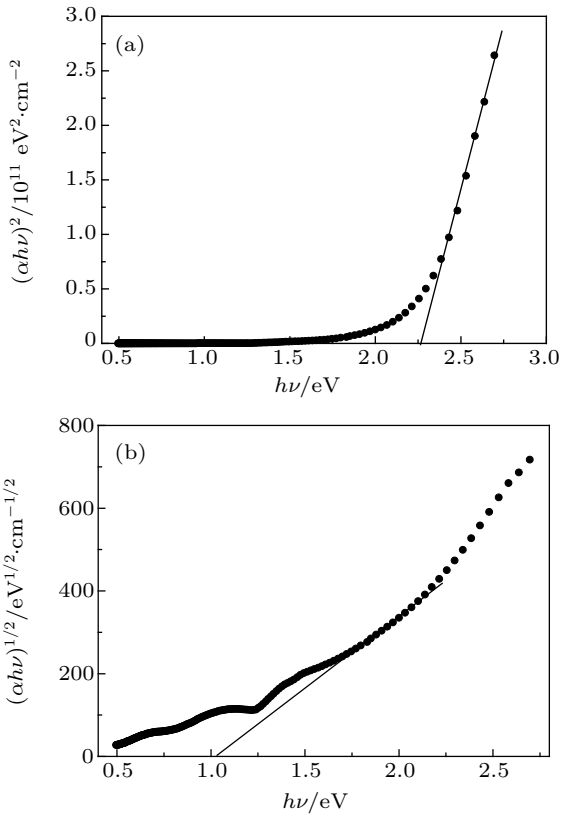


Fig. 9. Photon energy dependences of (a) $(\alpha h\upsilon)^2$ and (b) $(\alpha h\upsilon)^{1/2}$ of Cu_2S thin film.

Table 2. Energy gap values of Cu_2S film.

Sample	E_g^{dir}/eV	E_g^{ind}/eV	Reference
Thin film	2.26	1.03	present work
Thin layer	1.83	1.21	[24]
Thin layer	1.7	1.05	[25]
Thin film	2.1	1.4	[26]

3.3. Electrical characterizations

The values of dark electrical resistivity ρ are measured for Cu_2S films with thickness values ranging from 113 nm to 453 nm in a temperature range of 303 K–423 K. Figure 10 shows the variations of dark electrical resistivity with film thickness at different temperatures. As illustrated in Fig. 10,

the resistivity decreases with the increasing of film thickness, which is in accordance with the typical results for semiconducting films.[27] Sondheimer,[28] and Kimr[29] have analyzed the thickness dependence of electrical resistivity of thin film with consideration of the surface scattering of charge carriers. Tellier[30] has derived a simple analytical expression for the electrical resistivity as a function of thickness. According to this model, the film resistivity is simply given by

$$\rho = \rho_{\mathrm{B}}[1 + 3l_{\mathrm{o}}(1-p)/8d], \tag{9}$$

where ρ_{B} is the electrical resistivity of the infinite thick film and is named bulk resistivity, l_{o} is the mean free path and p is the proportion of electronelastic scattering. Assuming that all scatterings at film boundaries are inelastic ($p = 0$), equation (9) becomes the following equation

$$\rho \cdot d = \rho_{\mathrm{B}} \cdot d + (3/8) l_{\mathrm{o}} \rho_{\mathrm{B}}. \tag{10}$$

The values for the bulk resistivity and mean free path can be obtained by plotting the relation between $\rho \cdot d$ versus d, as shown in Fig. 11. The figure shows straight lines at different temperatures. The slope gives the bulk resistivity, ρ_{B}, and from the intercept the values of mean free path, l_{o}, can be determined for different temperatures. The calculated values are listed in Table 3.

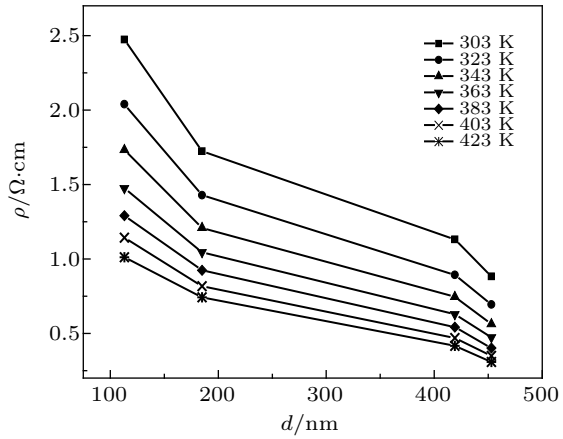


Fig. 10. Thickness dependences of dark electrical resistivity ρ at different temperatures for Cu_2S thin films.

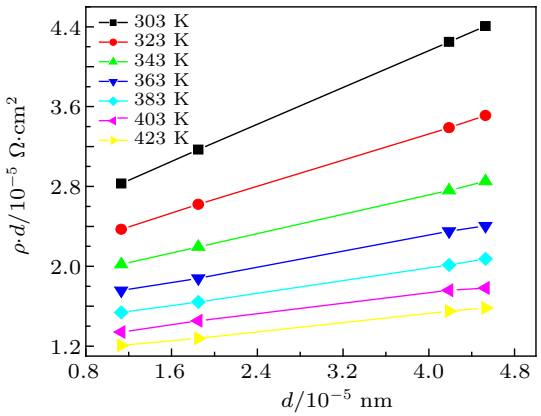


Fig. 11. (color online) Plots of $\rho \cdot d$ versus d at different temperatures for Cu_2S thin films.

Table 3. (color online) Values of bulk resistivity and mean free path at different temperatures for Cu_2S thin films.

Temperature/K	Bulk resistivity ρ_{B}/Ω·cm	Mean free path/μm
303	0.46	1.33
323	0.33	1.60
343	0.24	1.91
363	0.19	2.11
383	0.16	2.26
403	0.13	2.46
423	0.11	2.60

The temperature dependences of the dark electrical resistivity of Cu_2S films are studied to determine the thermal activation energy. Figure 12 shows the variations of ρ with temperature at different film thickness values. It is observed that, for each film thickness, the dark resistivity decreases with the increase in temperature. The temperature dependence of resistivity is expressed as follows:

$$\rho = \rho_{\mathrm{o}} \exp(\Delta E / k_{\mathrm{B}} T), \tag{11}$$

where ρ_{o} is a constant, ΔE is the thermal activation energy of the free charge carriers, and k_{B} is the Boltzmann's constant. Figure 13 presents the relations between $\ln\rho$ and $1000/T$ for different thickness values of Cu_2S films. As shown in the figure, there is a linear relation between $\ln\rho$ and $1000/T$ of Cu_2S films. The corresponding activation energies are calculated and listed in Table 4.

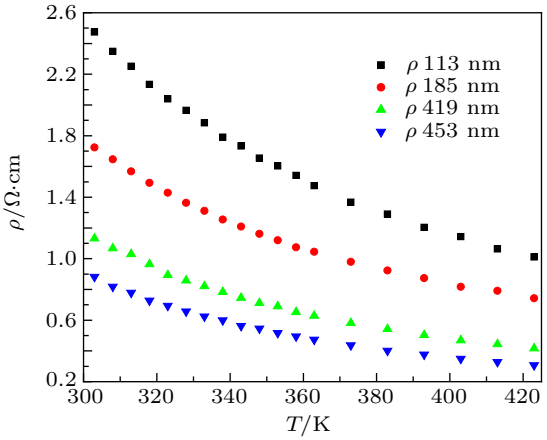


Fig. 12. (color online) Temperature dependences of dark electrical resistivity ρ at different thickness values for Cu_2S thin films.

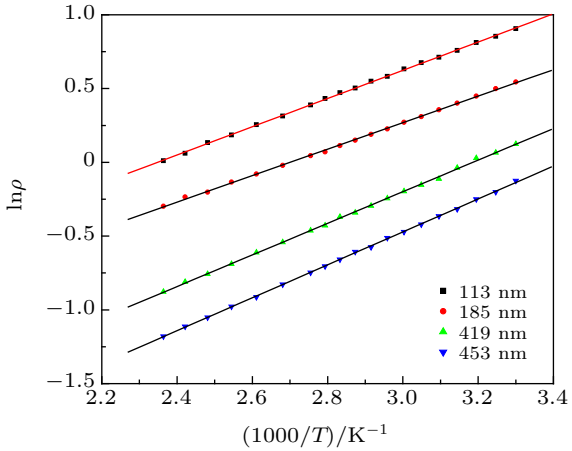


Fig. 13. (color online) Plots of $\ln\rho$ versus $1000/T$ at different thickness values for Cu_2S thin films.

Table 4. Activation energy values for Cu_2S thin films.

Film thickness/nm	Activation energy/eV
113	0.08
185	0.084
419	0.092
453	0.096

4. Conclusions

Copper sulfide thin films are deposited on different substrates using the thermal evaporation technique. The XRD pattern reveals that the film possesses a structure that matches the orthorhombic crystal system and has a chalcocite (γ-Cu_2S) phase. The AFM images reveal that the film exhibits nanoparticles with an average size of nearly 44 nm. The film shows high transmittance values at longer wavelengths in the near-infrared region. The spectral behavior of the reflectance reveals three peaks at 600, 780, and 1240 nm, respectively. The dispersion curve of the refractive index shows the anomalous dispersion at $\lambda < 1000$ nm and a normal dispersion at $\lambda > 1000$ nm. The values of single oscillator energy, dispersion energy, and infinite wavelength dielectric constant are calculated. The values of ε_L and N/m^* are found to be 4.79 and 4.84×10^{55} $m^{-3}\cdot kg^{-1}$, respectively. Direct- and indirect-allowed transitions are exhibited for Cu_2S thin film with energy gaps of 2.266 eV and 1.034 eV, respectively. The values of dark electrical resistivity measured for Cu_2S thin films are found to decrease with the increasing of film thickness. The values of bulk resistivity and the mean free path are determined for different temperatures. The temperature dependence of dark electrical resistivity presents a semiconductor behavior.

References

[1] Kassim A, Min H S, Siang L K and Nagalingam A 2011 *Chalcogenide Lettters* **8** 405

[2] Yamaamoto T, Kubota E, Taniguchi A, Dev S, Tanaka K and Osakada K 1992 *Chem. Mater.* **4** 570

[3] Sagade A A and Sharma K 2008 *Sensors and Actuators B: Chemical* **133** 135

[4] Allouche N K, Nasr T B, Guasch C N and Turki K 2010 *Comptes Rendus Chimie* **13** 1364

[5] Lim Y, Ok Y W, Tark S J, KangY, Kim D and Curr 2009 *Appl. Phys.* **9** 890

[6] Itoh K, Kuzuya T and Sumiyama K 2006 *Mater. Trans.* **47** 1953

[7] Tolansky S 1970 *Multiple-beam Interference, Microscopy of Metals*, (New York: Academic Press)

[8] Shklyarevski I N, Kornveeva T I and Zozula K N 1969 *Opt. Spect.* **27** 174

[9] El-Naggar A H 1999 *J. Phys. B: Condens. Matter* **11** 9619

[10] El-Nahass M M 1992 *J. Mater. Sci.* **27** 6592

[11] Bakry A M and El-NaggarA H 2000 *Thin Solid Films* **360** 293

[12] Seraphin B O 1979 *Solar Energy Conversions* (Berlin, Heidelberg, New York: Spring-Verlag)

[13] Freyland W, Goltzene A, Peter Grosse and Harbeke G 1983 *Physics of Non-Tetrahedrally Bonded Elements and Binary Compounds* (Berlin, Heidelberg, London, New York, Tokyo: Springer Verlag) p. 137

[14] Stendal A, Bechars Wilbrand U S, Stenzel O and Von Borczskowski C 1996 *J. Phys. B: At. Mol. Opt. Phys.* **29** 2589

[15] DiDomenico M and Wemple S H 1969 *J. Appl. Phys.* **40** 720

[16] Wemple S H and DiDomenico M 1971 *Phys. Rev. B* **3** 1338

[17] El-Nahass M M and Youssef T E 2010 *J. Alloys Compd.* **503** 86

[18] Ilican S and Caglar M Y 2007 *J. Opto. Electr. & Adv. Mater.* **9** 1414

[19] Wolaton A K and Moss T S 1963 *Proc. Roy. Soc.* **81** 5091

[20] Rajesh K R and Menon C S 2002 *Mater. Lett.* **53** 329

[21] Bardeen J, Blatt F J and Hall L T 1956 *Photoconductivity Conf.* (New York: Wiley) p. 146

[22] Tauc J, Grigorovici R and Vancu A 1996 *Phys. Status Solidi B* **15** 627

[23] Mulder B J 1973 *Phys. Status Solidi* **18** 633

[24] Shiozawa L R, Sullivan G A and Augustine F 1967 *Clevite Corporation*, Cleveland, Ohio, Contract No. AF **33** 615 5224

[25] Romoin M, Sorbier J P, Bretzner J F and Martinuzzi S 1969 *C. R. Acad. Sci. Ser. B* **268** 208

[26] Mulder B J 1973 *Phys. Status Solidi A* **132** 79

[27] Dhumure S S and Lokhands C D 1992 *Sol. Energy Mater. Sol. Cells* **28** 159

[28] Sondheimer E H 1952 *Adv. Phys.* **1** 1

[29] Kimr I H 2000 *Mater. Lett.* **44** 75

[30] Tellier C R 1978 *Thin Solid Films* **51** 311